Oncology and Translational Medicine
DOI 10.1007/s10330-020-0437-7
December 2020, Vol. 6, No. 6, P247–P257

ORIGINAL ARTICLE

Identification of potential immune-related prognostic biomarkers of lung cancer using gene co-expression network analysis*

Aixia Chen[1], Shengnan Zhao[2], Fei Zhou[1], Hongying Lv[1], Donghai Liang[1], Tao Jiang[1], Rui Liu[1], Lijin Zhu[1], Jingyu Cao[3], Shihai Liu[4], Hongsheng Yu[1] (✉)

[1] Department of Radiation Oncology, The Affiliated Hospital of Qingdao University, Qingdao 266000, China
[2] Department of Medcine Oncology, Qinghai University Affilated Hospital, Qinghai 810000, China
[3] Department of Hepatobilary and Pancreatic Surgery, The Affiliated Hospital of Qingdao University, Qingdao 266000, China
[4] Department of Central Laboratory, The Affiliated Hospital of Qingdao University, Qingdao 266000, China

Abstract

Objective The objective of this study was to identify new carcinogenetic hub genes and develop the integration of differentially expressed genes to predict the prognosis of lung cancer.

Methods GSE139032 microarray data packages were downloaded from the Gene Expression Omnibus for planning, testing, and review of data. We identified KRT6C, LAMC2, LAMB3, KRT6A, and MYEOV from a key module for validation.

Results We found that the five genes were related to a poor prognosis, and the expression levels of these genes were associated with tumor stage. Furthermore, Kaplan-Meier plotter showed that the five hub genes had better prognostic values. The mean levels of methylation in lung adenocarcinoma (LUAD) were significantly lower than those in healthy lung tissues for the hub genes. However, gene set enrichment analysis (GSEA) for single hub genes showed that all of them were immune-related.

Conclusion Our findings demonstrated that KRT6C, LAMC2, LAMB3, KRT6A, and MYEOV are all candidate diagnostic and prognostic biomarkers for LUAD. They may have clinical implications in LUAD patients not only for the improvement of risk stratification but also for therapeutic decisions and prognosis prediction.

Key words: lung adenocarcinoma (LUAD); bioinformatics; gene expression omnibus; gene expression profiling interactive analysis (GEPIA); prognosis; methylation

Abbreviations: LUAD, lung adenocarcinoma; GSEA, gene set enrichment analysis; NSCLC, non-small-cell lung cancer; WGCNA, weighted gene co-expression network analysis; MEs, module eigengenes; GS, gene significance; MS, module significance; KEGG, Kyoto Encyclopedia of Genes and Genomes; GO, gene ontology; CC, cellular component; MF, molecular function; BP, biological process; GEPIA, gene expression profiling interactive analysis; HPA, Human Protein Atlas; TIMER, Tumor Immune Estimation Resource; TCGA, The Cancer Genome Atlas; OS, overall survival; PF, first progression; PPS, post-progression survival; IHC, immunohistochemical

Received: 15 June 2020
Revised: 13 October 2020
Accepted: 8 November 2020

Lung cancer is the most frequently diagnosed type of cancer, accounting for 11.6% of all cancer cases, and is a leading cause of cancer morbidity, representing 18.4% of all cancer-related deaths [1]. Non-small cell lung cancer (NSCLC) is the most prevalent type of lung cancer, and lung adenocarcinoma (LUAD) is the most common subtype of NSCLC, representing almost half of lung cancer diagnoses [2]. Standard treatment for LUAD is surgical resection and chemotherapy, which improves survival rates by 5%–10% [3]. Many treatment options exist for LUAD; however, appropriate treatment usually depends on the stage of LUAD. Five-year survival rates are low and stage-dependent [3]. It has been reported that the number of CD133+ cells, which can increase drug

✉ Correspondence to: Hongsheng Yu. Email: qdyuhs@126.com
* Supported by a grant from the Chinese Society of Clinical Oncology (No. Y-HR2018-293 and Y-HR2018-294).
© 2020 Huazhong University of Science and Technology

resistance and the likelihood of tumor recurrence, are enhanced by the chemotherapeutic agent, cisplatin [4]. Early identification of LUAD through the discovery of relevant tumor biomarkers is urgently needed to improve prognoses [5–6].

A weighted gene co-expression network analysis (WGCNA) was used to identify correlations in gene patterns. We constructed a free-scale gene co-expression network to discover modules with highly correlated genes. Accordingly, we discuss here potential biomarkers of lung cancer to improve patient prognosis via a systematic biological method using WGCNA.

Materials and methods

Data procession and construction of co-expression network

Gene expression dataset GSE139032 (https://www.ncbi.nlm.nih.gov/geo/query/acc.cgi?acc=GSE139032), including 77 lung adenocarcinomas and 77 matched non-malignant lung samples (Illumina HumanMethylation27 BeadChip), were downloaded from the Gene Expression Omnibus [7]. Sangerbox (http://www.sangerbox.com), a free online tool for data analysis, was utilized to analyze sample information and dataset matrices. The top 50% of the most variable genes (7239) from the dataset (14 477 genes) were chosen by analysis of variance. Sangerbox was used to perform WGCNA, and study-specific parameters and WGCNA rationale are as follows [8].

First, a co-expression network was constructed with Pearson correlation coefficients *i* and *j* representing the expression levels of the *i*th and *j*th genes, respectively.

$$S_{ij} = |1 + cor(x_i + y_i)/2|$$

Second, the co-expression similarity was transformed into the adjacency according to the following equation:

$$a_{ij} = |(1 + cor(x_i + y_i))/2|^{\beta}$$

β: soft thresholding, which revealed the adjacency of a signed network [9]. We selected a soft threshold parameter power of β = 7 to build an approximately scale-free network to balance the scale-free network properties.

Third, the topological overlap measure (TOM) transformation was calculated from the adjacency matrix using

$$TOM = (\sum_{\mu \neq ij} \alpha_{i\mu}\alpha_{\mu j} + \alpha_{ij}) / (min(\sum_{\mu} \alpha_{i\mu} + \sum_{\mu} \alpha_{j\mu}) + 1 - \alpha_{ij})$$

to further convert the adjacency matrix of the 7239 genes from the co-expression network to the screening function module [10].

Screening of clinically significant modules

Module eigen genes (MEs) represent all genes in a specific module, which were screened for the identification of clinically relevant modules that correlate to a specific cancer type. Clinical traits, such as tumor stage and tumor grade, were calculated for each ME. Gene significance (GS) was utilized in the linear regression to quantify the relevance of the gene and clinical features [8]. The average absolute GS in a specific module was measured using module significance.

Functional enrichment analysis of gene ontology and KEGG

DAVID (https://david.ncifcrf.gov/), an online public web server, was used to characterize and manipulate gene lists by mining high-throughput genomic data and performing gene ontology (GO) and KEGG signaling pathway enrichment analysis. Cellular component (CC), molecular function (MF), and biological process (BP)were the three categories included in the ontology. A *P*-value < 0.05 was considered statistically significant.

Hub gene selection and validation

Gene connectivity was measured using the absolute value of Pearson's correlation, defined by module connectivity (cor. Gene module membership > 0.8) and clinical connectivity (cor. genetrait significance > 0.2). Gene expression profiling interactive analysis (GEPIA) was utilized to validate the central hub genes of LUAD. Immunohistochemistry of the five genes identified was performed using the Human Protein Atlas (HPA) (http://www.proteinatlas.org), which showed that the genes were upregulated in tumors.

Methylation analyses of hub genes

The human disease methylation database (DiseaseMeth version 2.0, http://biobigdata.hrbmu. edu.cn/diseasemeth/) contains methylome information from high-throughput microarray and sequencing studies of human methylation and shows DNA methylation abnormalities for human diseases in a case-control or disease-disease format [11–12].

Differences in the methylation levels of hub genes in cancerous lung tissues were compared with those in healthy lung tissues using the cBioPortal for Cancer Genomics (https://www.cbioportal.org/). Genetic changes associated with the hub genes were investigated to explore the associations between mRNA expression and DNA methylation in lung cancer using a large-scale cancer genome database.

Evaluation of the immunological infiltrate

To study the relationship between hub gene expression and immune cell infiltration, we used the online TIMER tool [13–14]. Samples (10 897) from a wide variety of cancers available from The Cancer Genome Atlas (TCGA) were used to study the interaction between hub gene expression and immune cell tumor infiltration.

Gene set enrichment analysis of hub genes

GSEA 3.0 software was used to analyze the hub genes

associated with immune infiltration of a variety of biological function gene sets in lung cancer.

Statistical analysis

WGCNA was performed using the Sangerbox platform (version 1.0.9) based on R software version 3.4.3. We utilized the Kaplan-Meier method to perform survival analysis using the log-rank test. The independent samples *t*-test for data comparison was performed by GEPIA. *P*-values < 0.05 (two-sided) were considered statistically significant.

Results

Weighted co-expression network building and key modules recognition

The coefficient and average association of Pearson's correlation were used to cluster the GSE139032 sample based on the WGCNA packages in R (Fig. 1 and 2). After transforming the co-expression similarity matrix, we computed the TOM to identify modules utilizing the dynamic tree cut method (Fig. 2c). WGCNA was performed to collect information for a co-expression network [9]. The soft threshold parameter power of β = 7 was selected to balance the scale-free nature of the network for a network that will be approximately scale-free (Fig. 2a and 2b). Using the average hierarchical linkage, 11 modules were identified. The turquoise module was selected as the clinically meaningful unit

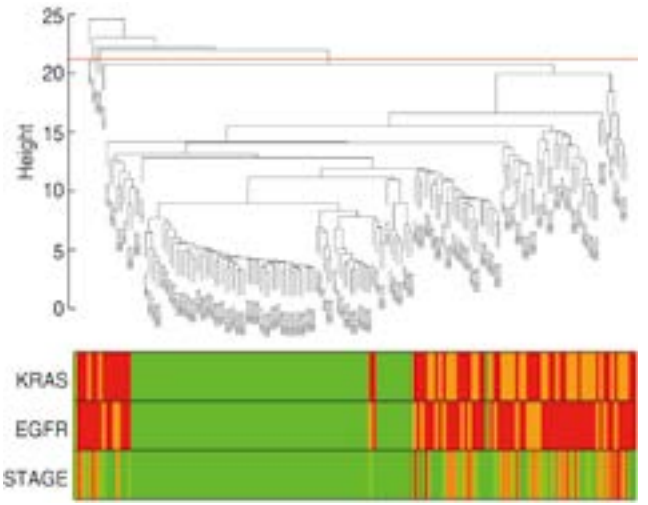

Fig. 1 Clustering dendrogram of 152 samples

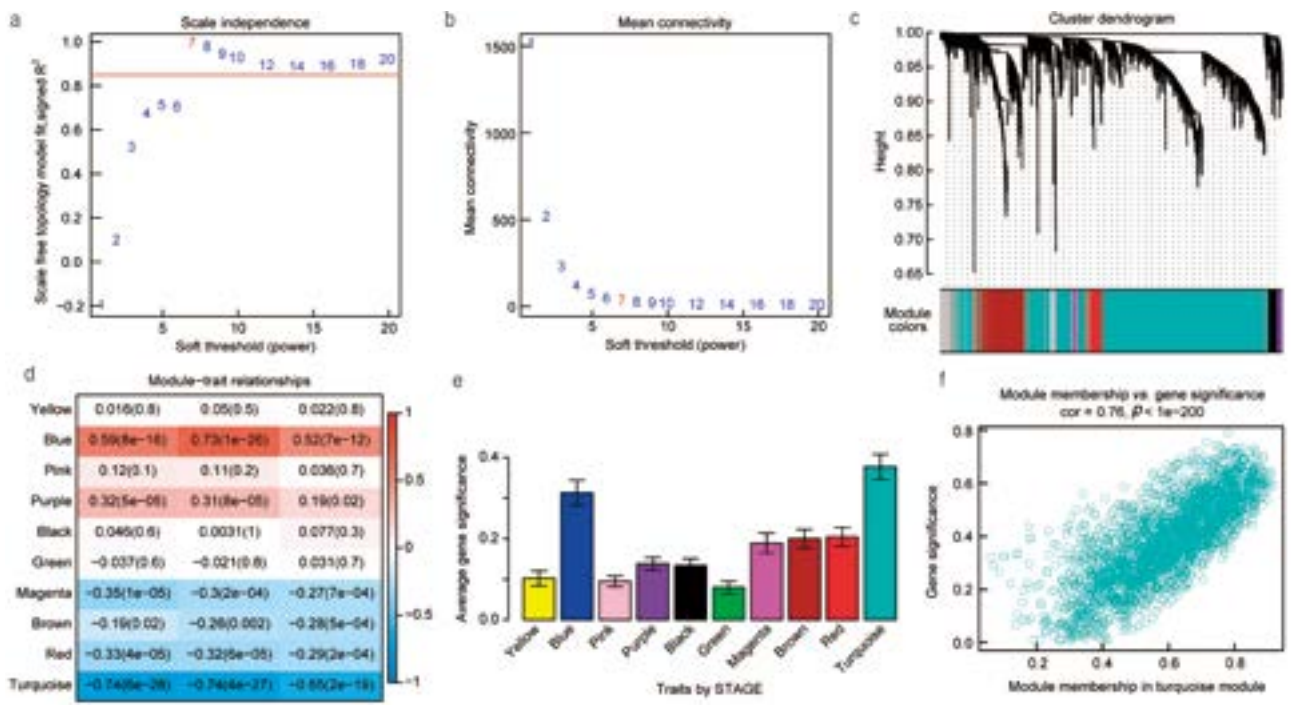

Fig. 2 Identification of modules related to clinical traits of LUAD through WGCNA. (a) Scale-free fit index analysis for a variety of soft threshold strengths (β). (b) Mean connectivity study for a number of soft thresholds. All modules were related to the respective LUAD clinical characteristics that were screened. (c) Gene dendrogram of differentially expressed genes obtained through clustering as a measure of dissimilarity (1-TOM). Each branch represents a single gene in the dendrogram. A specific color signifies a single module containing closely conserved genes. (d) Connection of the clinical phenotype of LUAD and consensus module eigengenes. (e) Bar graphs indicating the importance and errors of the individual modules across all modules associated with the LUAD tumor stage. (f) Scatter plot for the relationship between the significance of the gene and the membership of the gene module in the turquoise module. Every circle is a gene

owing to its close interaction with tumor stage (Fig. 2d) and the highest tumor stage association (Fig. 2d).

Functional enrichment analysis

GO and KEGG pathway enrichment analyses were performed. Functional groups included three parts (CC, MP, and BP) to analyze GO enrichment. Enrichment of genes in the CC group from the turquoise module mainly included the extracellular region, extracellular space, integral component of the plasma membrane, extracellular exosome, plasma membrane, cornified envelope, intermediate filament, apical plasma membrane, and blood microparticle. The genes from the module in the MF group were chiefly enriched in structural molecule activity, iron ion binding, CC chemokine receptor binding, serine-type endopeptidase activity, serine-type peptidase activity, calcium ion binding, chemokine activity, serine-type endopeptidase inhibitor activity, cytokine activity, and heme-binding. The BP group included clinically significant genes in the following modules: keratinization, immune response, peptide cross-linking, neutrophil chemotaxis, keratinocyte differentiation, innate immune response, monocyte chemotaxis, inflammatory response, epidermis development, and lymphocyte chemotaxis (Fig. 3). Hub genes from the turquoise module were enriched in the KEGG pathway as follows: cytokine receptor interaction, hematopoietic cell lineage, systemic lupuserythematosus, pancreatic secretion, carbohydrate digestion and absorption, neuroactive ligand-receptor interaction, complement and coagulation cascades, rheumatoid arthritis, fat digestion and absorption, and toll-like receptor signaling pathways.

Hub gene selection and validation

In terms of cut-off criteria $|MM| > 0.8$ and $|GS| > 0.2$, we identified 2496 hub genes from the turquoise unit. A

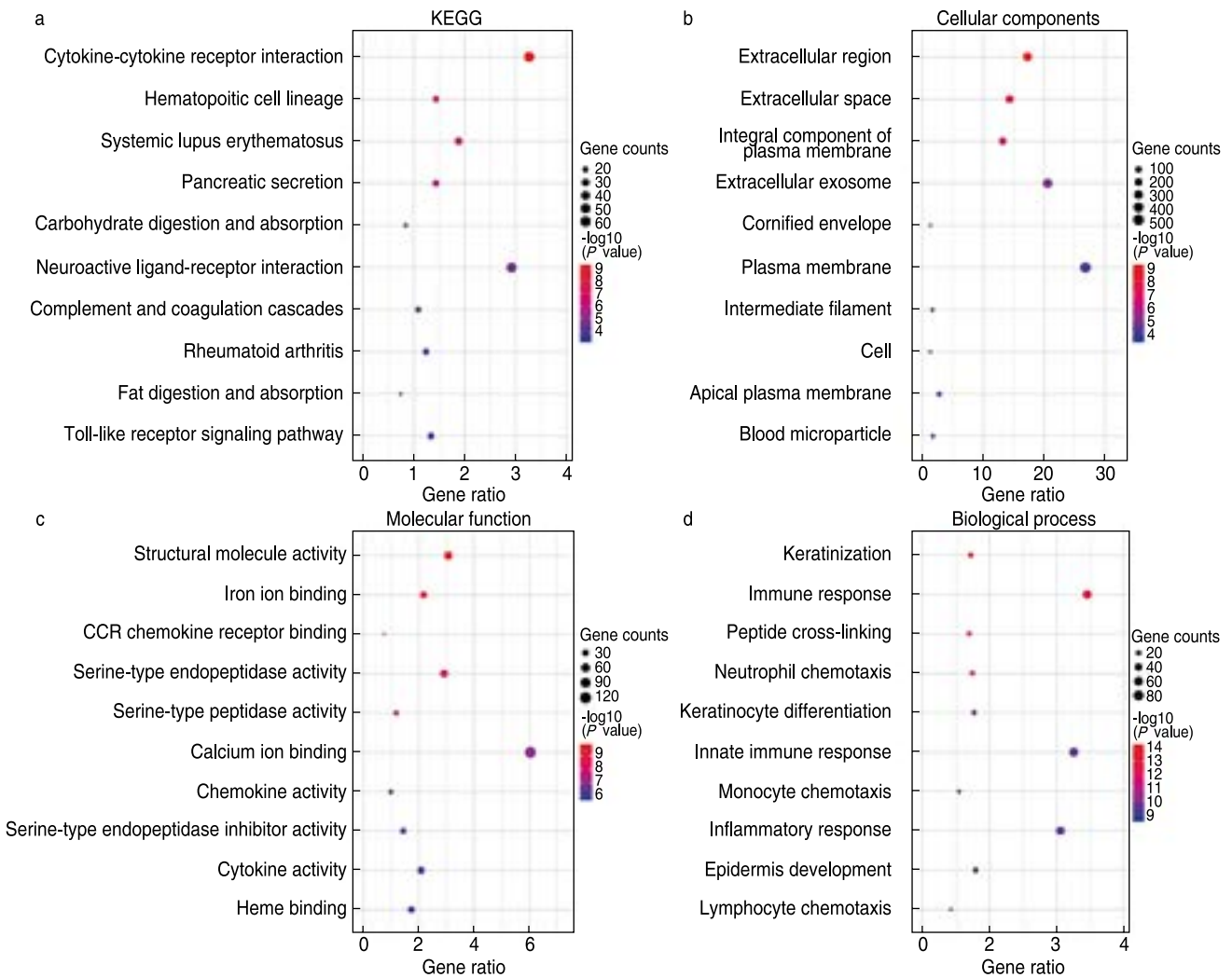

Fig. 3 The enrichment analyses of KEGG and GO pathways for all turquoise genes. An analysis of the (a) KEGG pathway of turquoise genes; (b) cellular components; (c) molecular function; and (d) biological process

Kaplan-Meier plotter was used to estimate the clinical prognostic significance of the hub genes. We found five genes (*MYEOV*, *LAMC2*, *LAMB3*, *KRT6C*, and *KRT6A*) that were negatively related to overall survival (OS) and first progression. *MYEOV, LAMC2, KRT6C,* and *KRT6A* were associated with post-progression survival (PPS). *LAMB3* was not associated with PPS (Fig. 4). GEPIA revealed a substantially higher level of expression of these five genes in tumor tissues than innormal tissue (Fig. 5a–5e). However, in advanced tumor stages,

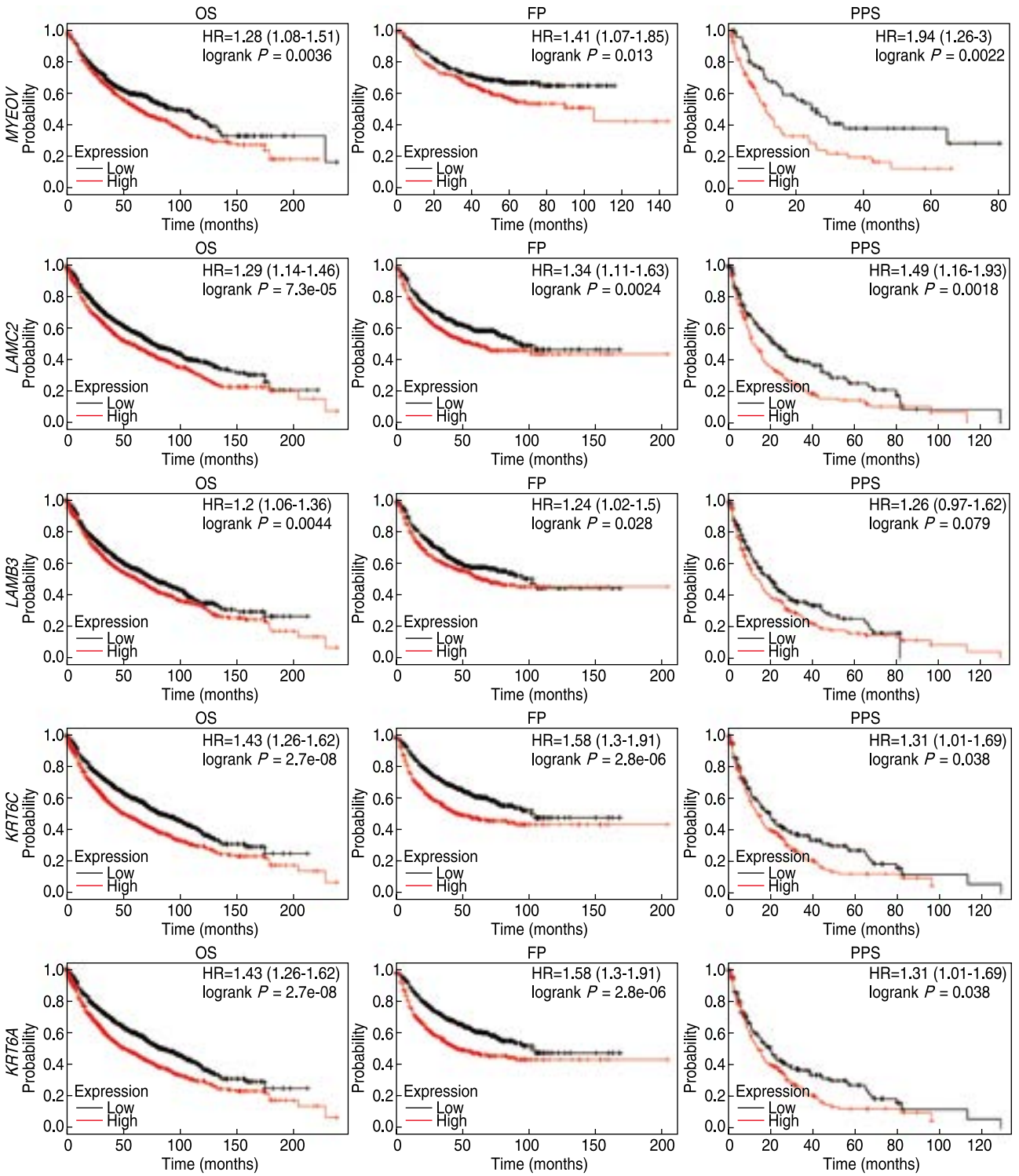

Fig. 4 Survival analysis using the Kaplan-Meier curve of *MYEOV*, *LAMC2*, *LAMB3*, *KRT6C*, and *KRT6A* in LUAD patients. HR, hazard ratio

based on a GEPIA cancer stage analysis, the expression levels of these five genes were found to be completely unregulated (Fig. 5f–5j). To estimate the expression of the proteins corresponding to the genes, the Protein Atlas

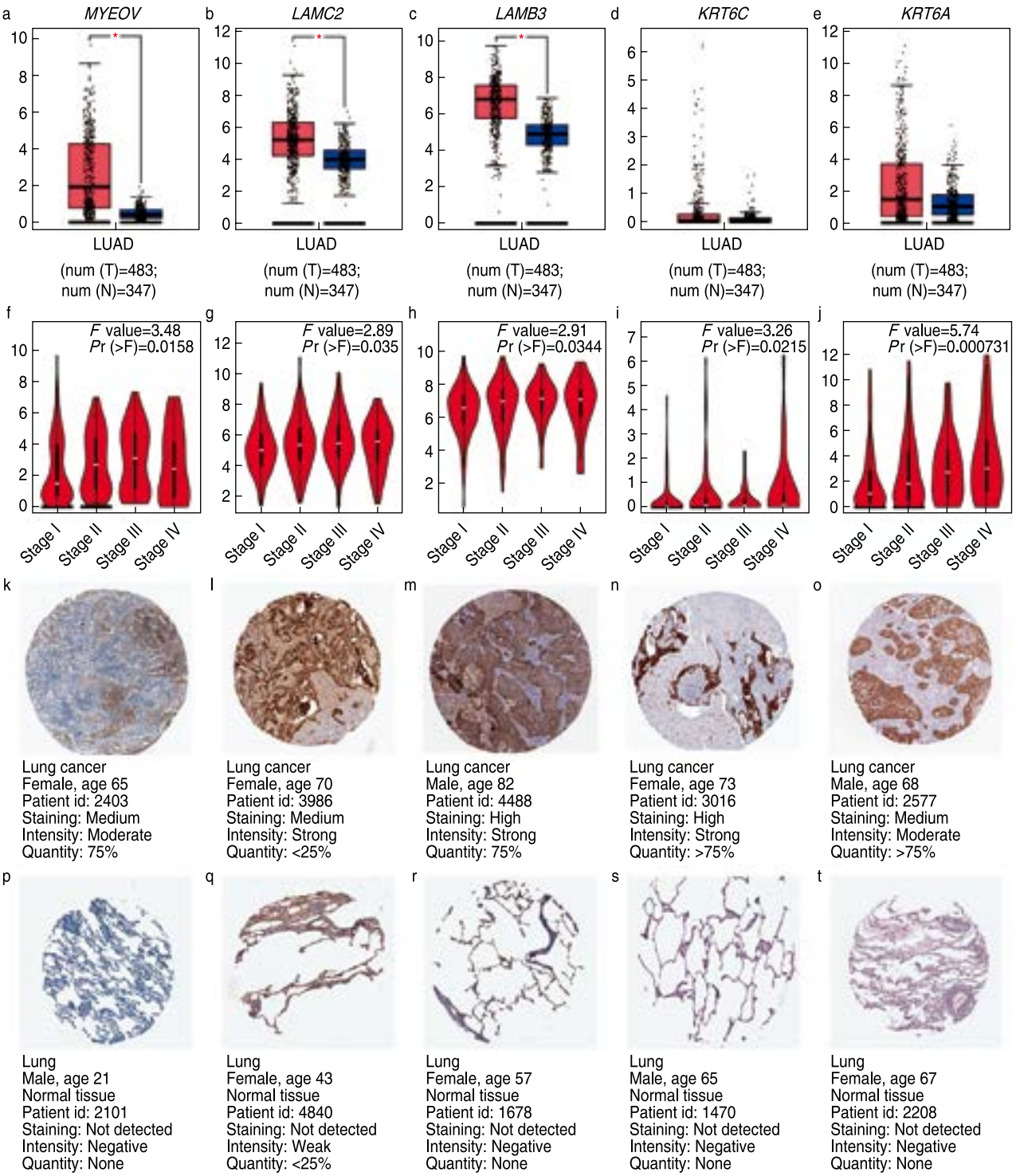

Fig. 5 (a–e) Expression of the five hub genes in LUAD and normal tissues ($P < 0.01$) from GEPIA. T: tumor, N: normal. (f–j) Correlation between expression of the five hub genes and tumor stage in LUAD using GEPIA. $P < 0.05$ represented a statistical difference. (k–t) Immunohistochemistry of the five hub genes in LUAD based on the Human Protein Atlas. (k and p) *MYEOV;* (l and q) *LAMC2;* (m and r) *LAMB3;* (n and s) *KRT6C;* (o and t) *KRT6A*. The top row is cancerous and the bottom row is normal lung tissue.

database (https://www.proteinatlas.org/) was used for immunohistochemistry (IHC) (Fig. 5k–5t).

Association between methylation and hub gene expression

The association between the expression of the five hub genes and their methylation status were analyzed to identify possible mechanisms for upregulation in lung tissues. A review of the human disease methylation databases (DiseaseMeth version 2.0) revealed that the mean levels of methylation in LUAD were significantly lower than those in healthy lung tissue for *MYEOV, LAMC2, LAMB3, KRT6C*, and KRT6A (Fig. 6a–6e). Fig. 6f–6j shows the correlation between mRNA expression and DNA methylation expression in the TCGA LUAD patient dataset. The negative correlations between them indicated that mRNA expression levels of these genes were maintained by methylation (cBioPortal dataset

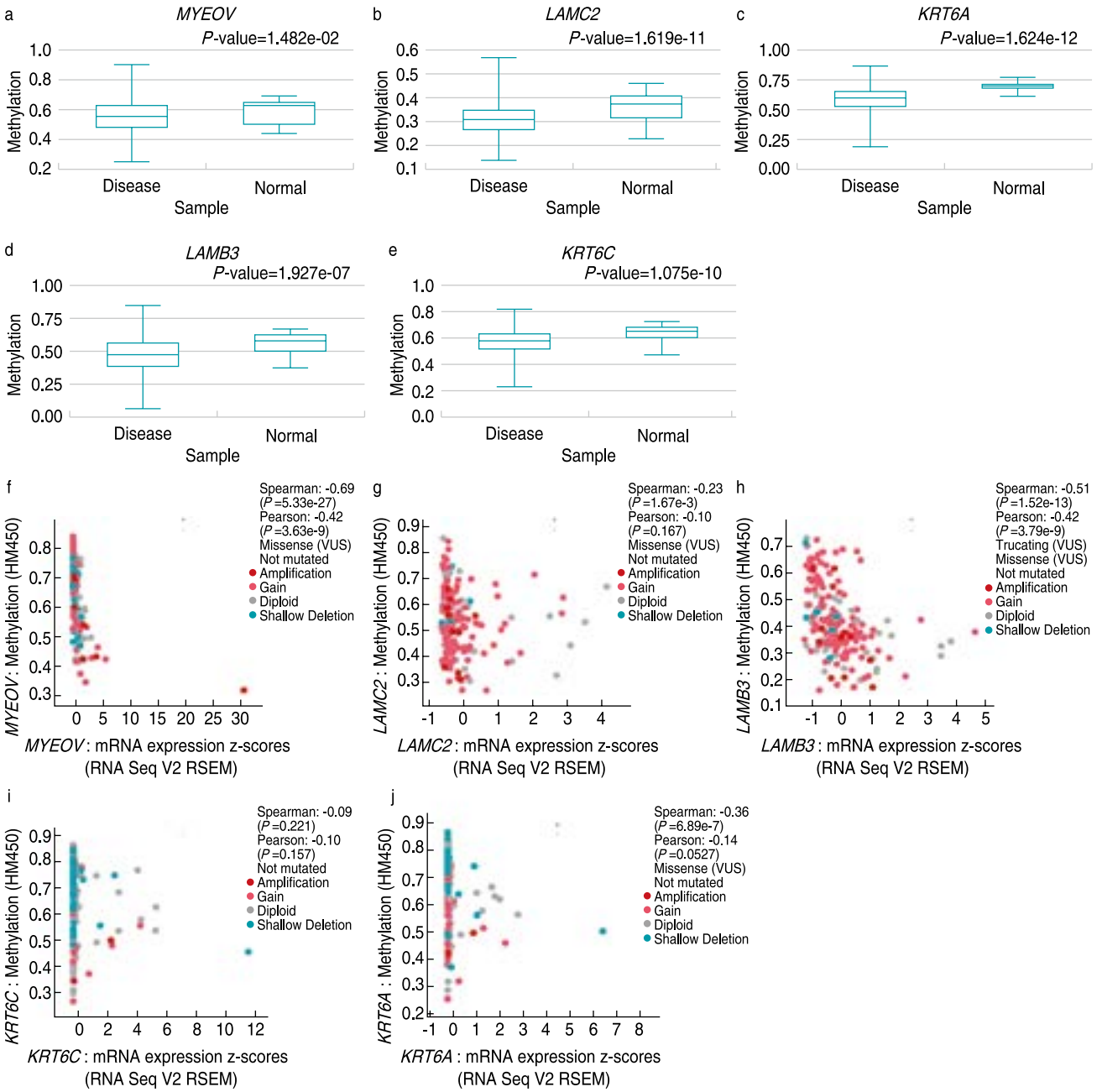

Fig. 6 Methylation analyses of the hub genes in LUAD. (a–e) The methylation levels of the genes in tumor and normal tissues. (a) *MYEOV;* (b) *LAMC2;* (c) *KRT6A;* (d) *LAMB3;* (e) *KRT6C*. (f–g) Relationship between mRNA expression and DNA methylation in the TCGA data set of hub genes. (f) *MYEOV*; (g) *LAMC2*; (h) *LAMB3*; (i) *KRT6C*; (j) *KRT6A*

https://www.cbioportal.org/).

Association between hub gene expression and immune infiltration

For the lung cancer hub genes, we used the TIMER platform to investigate possible associations between gene expression and immune infiltration. *MYEOV*, *LAMB3*, *LAMC2*, *KRT6C*, and *KRT6A* were positively correlated with tumor purity and B cells (Fig. 7). CD4+ T cells, CD8+ T cells, neutrophils, macrophages, and dendritic cells showed no or low correlation with *MYEOV*, *LAMB3*, *LAMC2*, *KRT6C*, and *KRT6A*.

Relationship between hub genes and immune signaling pathway

GSEA was performed to investigate the functions of *MYEOV*, *LAMB3*, *LAMC2*, *KRT6C*, and *KRT6A*. *KRT6A* was enriched in "peroxisome," "FC epsilon RI signaling pathway," and "complement and coagulation cascade" pathways (Fig. 8). *KRT6C* was enriched in "antigen processing and presentation," "cytosolic and sensing pathway," and "Toll-like receptor signaling pathway." *LAMB3* was enriched in "calcium signaling pathway" and "FC epsilon RI signaling pathway." *MYEOV* was enriched in "RIG-I-like receptor signaling pathway." *LAMC2* was enriched in "dorsoventral axis formation"

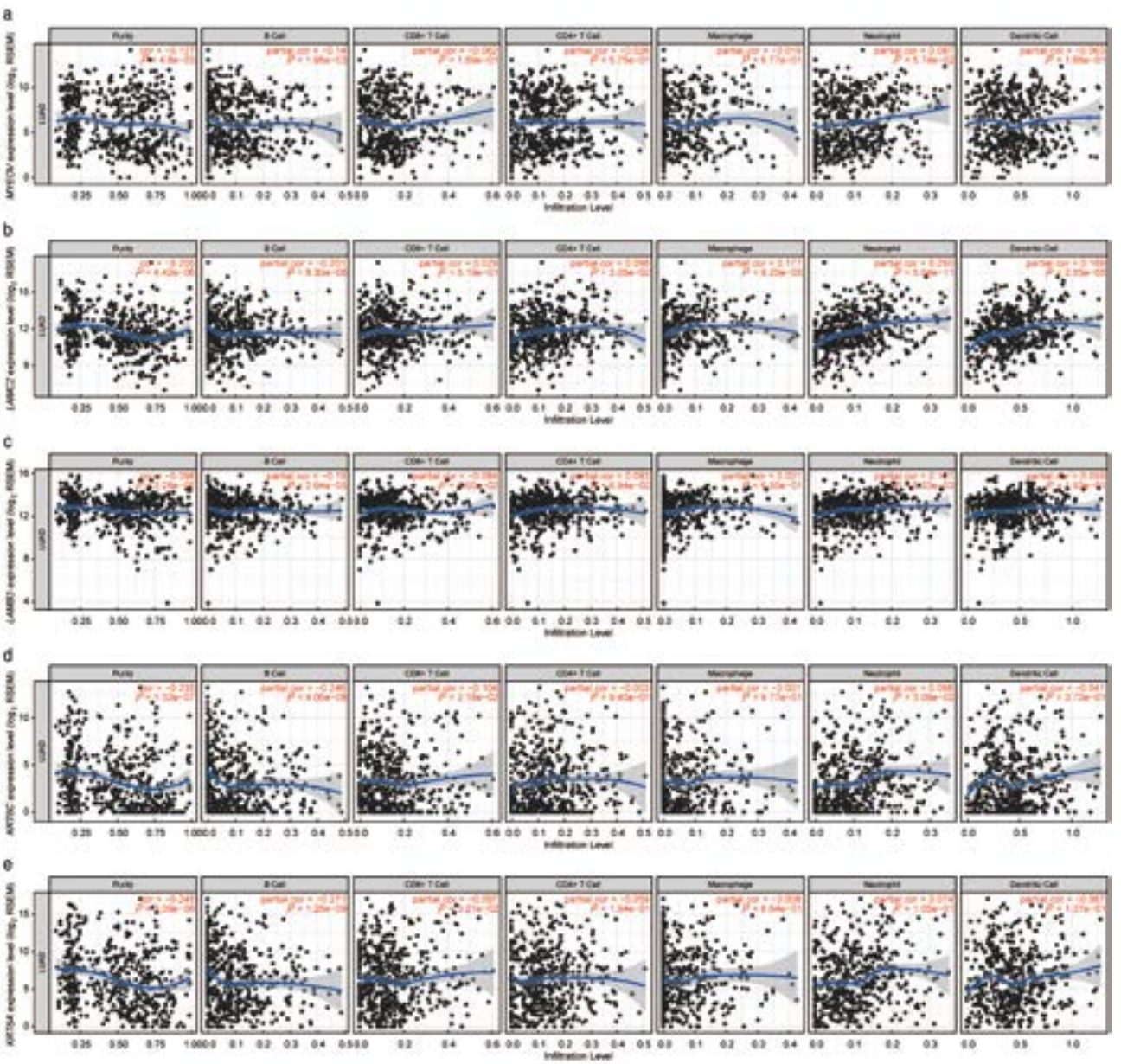

Fig. 7 LUAD immune infiltration connected with hub gene expression. (a) *MYEOV*; (b) *LAMC2;* (c) *LAMB3;* (d) *KRT6C;* (e) *KRT6A*. A *P*-value of < 0.05 was considered statistically significant. Each dot corresponds to a sample in the dataset of TCGA-PRAD

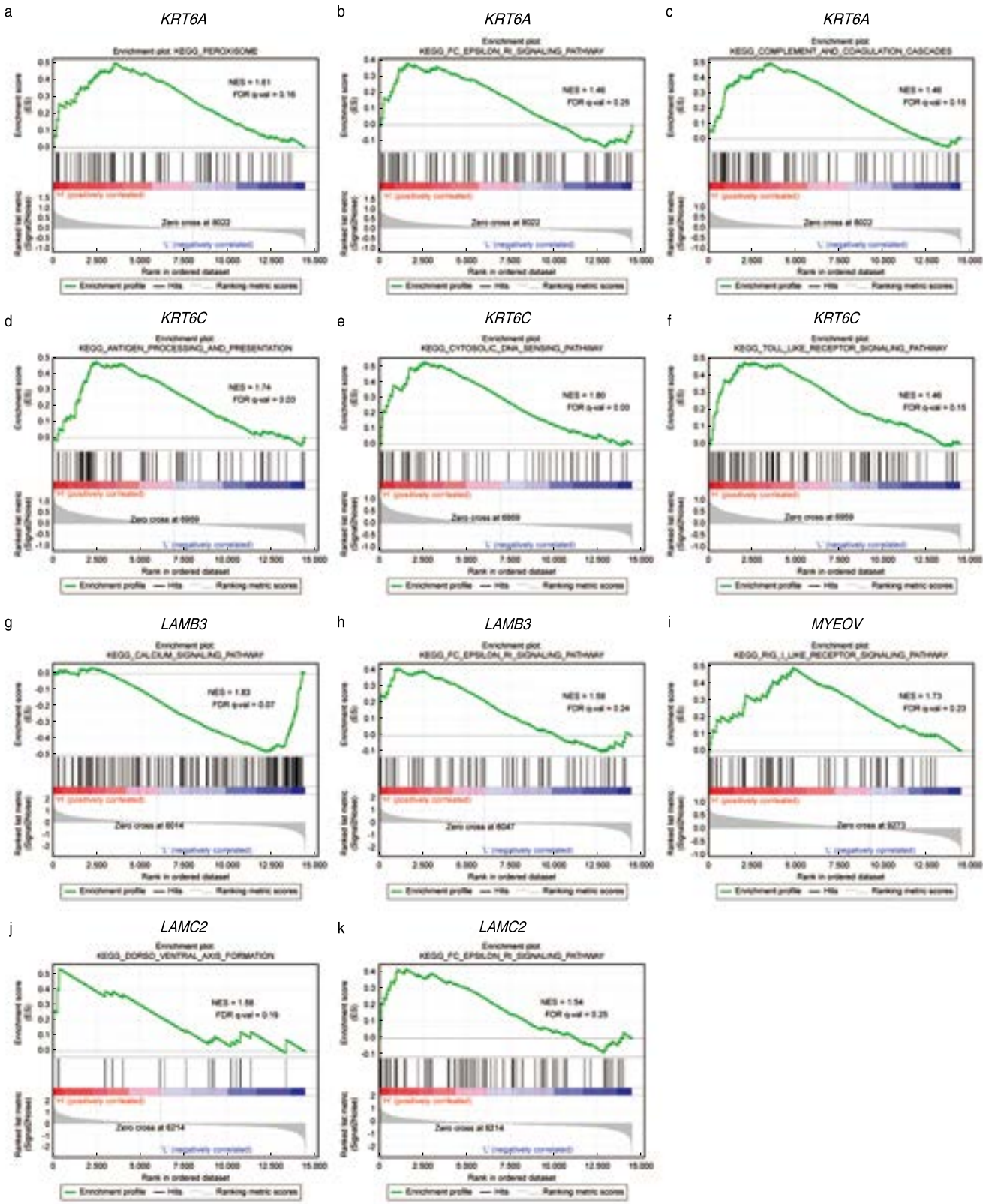

Fig. 8 Gene set enrichment analysis (GSEA) of significant gene sets in accordance with the GSEA enrichment score of the five hub genes. (a–c) *KRT6A;* (d–f) *KRT6C;* (g–h) *LAMB3;* (i) *MYEOV;* (j–k) *LAMC2*

and "FcEpsilonRI signaling pathway."

Discussion

Survival after diagnosis of NSCLC improved from 2013 to 2016 in the United States and is related to the use of targeted therapies [15]. As a molecularly heterogeneous disease, understanding the biology is critical for the treatment of lung cancer. The treatment of lung cancer has transformed owing to the identification of targetable gene alterations and the utilization of individualized therapy resulting from tumor genotyping. In comparison to those without targeted therapies, the survival of patients who are treated with genotype-directed therapy has improved [16]. New diagnostic and prognostic markers that might support the treatment of lung cancer are crucial.

Our study used the WGCNA approach to construct co-expression modules of genes related to lung cancer. In comparison to traditional microarray expression profiling, WGCNA focused more on a batch of gene modules rather than on individual genes, which may avoid the drawbacks of treating genes separately and prevent missing the transcriptional molecular networks [17]. In our study, comprehensive bioinformatics analyses, including WGCNA, were used to screen five genes connected to the progression and prognosis of LUAD.

MYEOV is found in the chromosomal region (chr) 11q13.3, which is associated with carcinogenic amplification [18–19]. This region has been studied in various cancers, including colon [20], gastric [21], esophageal squamous cell [22], neuroblastoma [23], and multiple myeloma [24]. *MYEOV* is a prognostic factor in multiple myeloma [24]. The molecular mechanisms of carcinogenic amplification are still unclear.

Laminin-5 is a large molecule of α3, β3, and μ2 chains encoded by *LAMA3*, *LAMB3*, and *LAMC2*, respectively, and is necessary for cancer diagnosis. Outcomes for patients with stage I LUAD correlated with dysregulated LAMC2 protein expression [25–27]. Moreover, LAMB3 cleavage by membrane type-1-matrix metalloproteinase (MT1-MMP) [28] and matrilysin [29] was associated with increased carcinoma cell migration. Our results implied that *LAMC2* and *LAMB3* expression are upregulated in tumor tissues compared to that in healthy tissues and arerelated to advanced tumor stage (Fig. 5f–5j). However, the influence of *LAMC2* and *LAMB3* overexpression in lung cancer is unclear.

The most common proteins in exhaled breath condensate samples are KRT6C and KRT6A, and their expression levels in lung cancer tissues are high [30]. We found that KRT6C and KRT6A overexpression were associated with poorer prognosis and advanced tumor stage in LUAD (Fig. 4 and Fig. 5f–5j).

Our study had several limitations. First, as with most data mining methods, technical artifacts or tissue contaminations may have influenced our WGCNA results. Second, owing to HPA limitations, the immunohistochemical data shown were from an assortment of patient samples that may not be relevant for LUAD.

DiseaseMeth 2.0 and cBioPortal were also utilized to explore DNA methylation patterns that may have an aberrant expression in LUAD. In comparison to standard samples, *MYEOV*, *LAMB3*, *LAMC2*, *KRT6C*, and *KRT6A* were found to be hypomethylated and associated with the upregulation of the five hub genes observed in LUAD. DNA methylation abnormalities are significantly related to the oncogenic properties of alternative promoters [31]. Feinberg pointed out that DNA methylation is responsible for the occurrence of cancer progenitor cells [32]. DNA hypomethylation of promoter region melanoma-related CT antigen MAGE was associated with recrudescence in colorectal cancer and melanoma [33–34]. In breast and colorectal cancers, overexpression of P-cadherin is caused by hypomethylation of the promoter region of CDH3 and promotescell invasion, motility, and migration [35].

We used TIMER and GSEA for each hub gene to investigate biological functions. Tumor purity and B cells positively correlated with *MYEOV*, *LAMB3*, *LAMC2*, *KRT6C*, and *KRT6A*. In LUAD samples, no significant associations were found between these hub genes and other immune infiltrates. GSEA indicated that single hub genes were significantly enriched in immune pathways. Increased expression of T and B cells, such as adenocarcinoma B cells and CD8 cells, predicts OS in patients with LUAD [36]. Moreover, further research needs to be conducted to study the correlation between the hub genes and smokers carrying lung cancer, in terms of an increase in the development of squamous cell carcinoma. Deficient-type GSTM1 has been shown to increase the risk of squamous cell carcinoma development [37]. We believe that the five hub genes are mainly expressed in lung cancer cells and are related to B cell functions.

Conclusion

We identified five hub genes (*MYEOV*, *LAMB3*, *LAMC2*, *KRT6C*, and *KRT6A*) that were correlated with the development and prognosis of lung cancer and potentially regulated by epigenetic mechanisms. Additional research is required to demonstrate their contribution to the pathogenesis of lung cancer and confirm their utility as diagnostic and/or predictive biomarkers.

Acknowledgments

We thank the Gene Expression Omnibus and TCGA database for sharing large amounts of data.

Conflicts of interest

The authors indicated no potential conflicts of interest.

References

1. Bray F, Ferlay J, Soerjomataram I, *et al*. Global cancer statistics 2018: GLOBOCAN estimates of incidence and mortality worldwide for 36 cancers in 185 countries. CA Cancer J Clin, 2018, 68: 394–424.
2. Nesbitt JC, Putnam JB, Walsh GL, *et al*. Survival in early-stage non-small cell lung cancer. Ann Thorac Surg,1995, 60: 466–472.
3. Liang Y, Wakelee HA. Adjuvant chemotherapy of completely resected early stage non-small cell lung cancer (NSCLC). Transl Lung Cancer Res, 2013, 2: 403–410.
4. Li JH, Jiang M, Zhao XT, *et al*. Cisplatin selects for CD133+ cells in lung cancer cells. Oncol Transl Med, 2020, 6: 16–20.
5. Chan BA, Hughes BGM. Targeted therapy for non-small cell lung cancer: current standards and the promise of the future. Transl Lung Cancer Res, 2015, 4: 36–54.
6. Francis H, Solomon B. The current status of targeted therapy for non-small cell lung cancer. Intern Med J, 2010, 40: 611–618.
7. Edgar R, Domrachev M, Lash AE. Gene Expression Omnibus: NCBI gene expression and hybridization array data repository. Nucleic Acids Res, 2002, 30: 207–210.
8. Langfelder P, Horvath S. WGCNA: an R package for weighted correlation network analysis. BMC Bioinformatics, 2008, 9: 559.
9. Zhang B, Horvath S. A general framework for weighted gene co-expression network analysis. Stat Appl Genet Mol Biol, 2005, 4: Article 17. doi: 10.2202/1544-6115.1128. Epub 2005 Aug 12.
10. Yip AM, Horvath S. Gene network interconnectedness and the generalized topological overlap measure. BMC Bioinformatics, 2007, 8: 22.
11. Lv J, Liu HB, Su JZ, *et al*. DiseaseMeth: a human disease methylation database. Nucleic Acids Res, 2012, 40 (Database issue): D1030–D1035.
12. Xiong YC, Wei YJ, Gu Y, *et al*. DiseaseMeth version 2.0: a major expansion and update of the human disease methylation database. Nucleic Acids Res, 2017, 45 (D1): D888–D895.
13. Li B, Severson E, Pignon JC, *et al*. Comprehensive analyses of tumor immunity: implications for cancer immunotherapy. Genome Biol, 2016, 17: 174.
14. Li TW, Fan JY, Wang BB, *et al*. TIMER: A web server for comprehensive analysis of tumor-infiltrating immune cells. Cancer Res, 2017, 77: e108–e110.
15. Howlader N, Forjaz G, Mooradian MJ, *et al*. The effect of advances in lung-cancer treatment on population mortality. N Engl J Med, 2020, 383: 640–649.
16. Herbst RS, Morgensztern D, Boshoff C. The biology and management of non-small cell lung cancer. Nature, 2018, 553: 446–454.
17. Ivliev AE, Hoen PAC, Sergeeva MG. Coexpression network analysis identifies transcriptional modules related to proastrocytic differentiation and sprouty signaling in glioma. Cancer Res, 2010, 70: 10060–10070.
18. Hui ABY, Or YYY, Takano H, *et al*. Array-based comparative genomic hybridization analysis identified cyclin D1 as a target oncogene at 11q13.3 in nasopharyngeal carcinoma. Cancer Res, 2005, 65: 8125–8133.
19. Brown LA, Irving J, Parker R, *et al*. Amplification of EMSY, a novel oncogene on 11q13, in high grade ovarian surface epithelial carcinomas. Gynecol Oncol, 2006, 100: 264–270.
20. Moss AC, Lawlor G, Murray D, *et al*. ETV4 and Myeov knockdown impairs colon cancer cell line proliferation and invasion. Biochem Biophys Res Commun, 2006, 345: 216–221.
21. Leyden J, Murray D, Moss A, *et al*. Net1 and Myeov: computationally identified mediators of gastric cancer. Br J Cancer, 2006, 94: 1204–1212.
22. Janssen JWG, Imoto I, Inoue J, *et al*. MYEOV, a gene at 11q13, is coamplified with CCND1, but epigenetically inactivated in a subset of esophageal squamous cell carcinomas. J Hum Genet, 2002, 47: 460–464.
23. Takita J, Chen YY, Okubo J, *et al*. Aberrations of NEGR1 on 1p31 and MYEOV on 11q13 in neuroblastoma. Cancer Sci, 2011, 102: 1645–1650.
24. Moreaux J, Hose D, Bonnefond A, *et al*. MYEOV is a prognostic factor in multiple myeloma. Exp Hematol, 2010, 38: 1189–1198. e3.
25. Aumailley M, Bruckner-Tuderman L, Carter WG, *et al*. A simplified laminin nomenclature. Matrix Biol, 2005, 24: 326–332.
26. Kagesato Y, Mizushima H, Koshikawa N, *et al*. Sole expression of laminin gamma 2 chain in invading tumor cells and its association with stromal fibrosis in lung adenocarcinomas. Jpn J Cancer Res, 2001, 92: 184–192.
27. Moriya Y, Niki T, Yamada T, *et al*. Increased expression of laminin-5 and its prognostic significance in lung adenocarcinomas of small size. An immunohistochemical analysis of 102 cases. Cancer, 2001, 91: 1129–1141.
28. Udayakumar TS, Chen ML, Bair EL, *et al*. Membrane type-1-matrix metalloproteinase expressed by prostate carcinoma cells cleaves human laminin-5 beta3 chain and induces cell migration. Cancer Res, 2003, 63: 2292–2299.
29. Remy L, Trespeuch C, Bachy S, *et al*. Matrilysin 1 influences colon carcinoma cell migration by cleavage of the laminin-5 beta3 chain. Cancer Res, 2006, 66: 11228–11237.
30. López-Sánchez LM, Jurado-Gámez B, Feu-Collado N, *et al*. Exhaled breath condensate biomarkers for the early diagnosis of lung cancer using proteomics. Am J Physiol Lung Cell Mol Physiol, 2017, 313: L664–L676.
31. Takacs M, Banati F, Koroknai A, *et al*. Epigenetic regulation of latent Epstein-Barr virus promoters. Biochim Biophys Acta, 2010, 1799: 228–235.
32. Feinberg AP, Ohlsson R, Henikoff S. The epigenetic progenitor origin of human cancer. Nat Rev Genet, 2006, 7: 21–33.
33. Weber J, Salgaller M, Samid D, *et al*. Expression of the MAGE-1 tumor antigen is up-regulated by the demethylating agent 5-aza-2'-deoxycytidine. Cancer Res, 1994, 54: 1766–1771.
34. Kim KH, Choi JS, Kim IJ, *et al*. Promoter hypomethylation and reactivation of MAGE-A1 and MAGE-A3 genes in colorectal cancer cell lines and cancer tissues. World J Gastroenterol, 2006, 12: 5651–5657.
35. Paredes J, Albergaria A, Oliveira JT, *et al*. P-cadherin overexpression is an indicator of clinical outcome in invasive breast carcinomas and is associated with CDH3 promoter hypomethylation. Clin Cancer Res, 2005, 11: 5869–5877.
36. Iglesia MD, Parker JS, Hoadley KA, *et al*. Genomic analysis of immune cell infiltrates across 11 tumor types. J Natl Cancer Inst, 2016, 108: djw144.
37. Li JH, Zhang LN, Wang Y, *et al*. Association of genetic polymorphisms of GSTM1 and smoking status with lung cancer risk. Oncol Transl Med, 2019, 5: 249–256.

DOI 10.1007/s10330-020-0437-7

Cite this article as: Chen AX, Zhao SN, Zhou F, *et al*. Identification of potential immune-related prognostic biomarkers of lung cancer using gene co-expression network analysis. Oncol Transl Med, 2020, 6: 247–257.